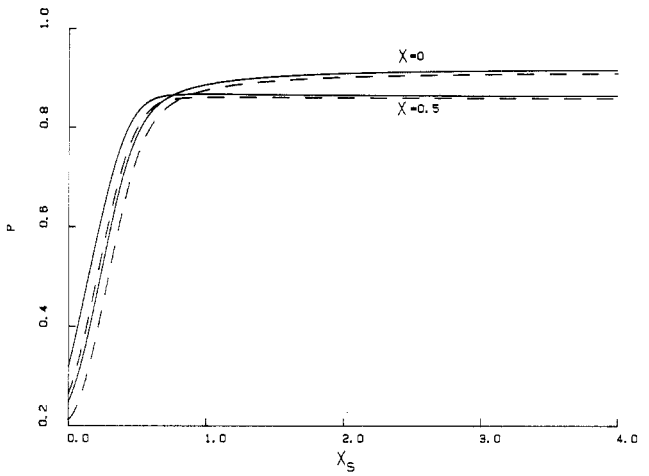

Figure 7. Bound fraction p as a function of χ_s for rings (—) and linear chains (- - -) for a Θ solvent (χ = 0.5) and a good solvent (χ = 0). r = 20 and $\phi_* = 10^{-4}$.

of linear chains and p of rings is always greater than p of linear chains. Polymer rings will be slightly more effectively anchored at an interface but will always form a thinner layer.

Conclusion

We have shown that the self-consistent field theory of Scheutjens and Fleer can be successfully adapted for the case of ring polymers. The results of these calculations emphasize the importance of tails in determining the adsorbed amount, the layer thickness, and the bound fraction.

Acknowledgment. We thank Timothy Heath, Brian Vincent, and Gerard Fleer for their continued interest and encouragement during this project.

References and Notes

(1) Cosgrove, T.; Vincent, B. *Adv. Colloid Interface Sci.* **1986**, *24*, 142.
(2) Scheutjens, J. M. H. M.; Fleer, G. J. *J. Phys. Chem.* **1979**, *83*, 1619.
(3) Scheutjens, J. M. H. M.; Fleer, G. J. *J. Phys. Chem.* **1980**, *84*, 178.
(4) Cohen Stuart, M. A.; Waajen, F. H. W. H.; Cosgrove, T.; Vincent, B.; Crowley, T. L. *Macromolecules* **1984**, *17*, 1825.
(5) Cosgrove, T.; Vincent, B.; Crowley, T. L.; Cohen Stuart, M. A. *ACS Symp. Ser.* **1984**, *240*, 147.
(6) Brown, J. F.; Slusarczuk, G. M. J. *J. Am. Chem. Soc.* **1965**, *87*, 931.
(7) Chen, Yi-Der *J. Chem. Phys.* **1981**, *74*, 2034.
(8) Higgins, J. S.; Ma, K.; Nicholson, L. K.; Hayter, J. B.; Dodgson, K.; Semlyen, J. A. *Polymer* **1983**, *24*, 793.
(9) Silberberg, A. *J. Chem. Phys.* **1968**, *48*, 2835.
(10) Roe, R. J. *J. Chem. Phys.* **1974**, *60*, 4192.
(11) DiMarzio, E. A.; Rubin, R. J.; *J. Chem. Phys.* **1971**, *55*, 4318.
(12) Whittington, S. G., private communication. Broadbent, S. R.; Hammersley, J. M. *Proc. Cambridge Philos. Soc.* **1957**, *53*, 629, 642.

Forward Depolarized Dynamic Light Scattering from Wormlike Chains

Sergio R. Aragón S.

Department of Chemistry, San Francisco State University, San Francisco, California 94132.
Received September 23, 1986

ABSTRACT: The forward depolarized light scattering correlation function is calculated for a dilute solution of polymers modeled as elastic wormlike chains in the free-draining limit. The polymer is represented hydrodynamically by an effective cylindrically symmetric body and characterized by a single end-over-end rotational diffusion coefficient, Θ. The correlation function for N polymer molecules is an infinite series of decaying exponentials of the form $C(t) = (N\beta^2/15)e^{-6\Theta t}\sum_{jk}a_{jk}b_{jk}(a)\exp[-D(x_j^4 + x_k^4)t/(2aL^2)]$, where β is the segment optical anisotropy, D is the translational diffusion coefficient, L is the contour length, and $a = \lambda L$ is the number of Kuhn lengths. The quantities $x_j \simeq (2j + 1)\pi/2$ are eigenvalues of the elastic bending problem. An important feature of the above result is the combination of rotational and flexural contributions to the time constants of the relaxation terms. The relative contribution of each of these processes is a function of flexibility. Comparison with Brownian dynamics simulations indicates that the weights are greatly affected by the neglect of hydrodynamic interactions in the theory. Nevertheless, this equation is the first calculation of the depolarized scattering from a semiflexible molecule that has the correct rigid rod limit. It should also be applicable for the description of the field-free decay of the birefringence from molecules without a permanent dipole moment. The theory is in good agreement with experimental data from DNA restriction fragments.

I. Introduction

The wormlike coil model of Kratky and Porod[1] is one of the simplest one-parameter descriptions available for stiff linear polymer chains. the attractiveness of the model stems from its ability to span the whole range of flexibilities from the random coil to the rigid rod. The properties of the polymer chain can be expressed in terms of the ratio, a, of the Kuhn statistical segment length, λ^{-1}, to the contour length, L. The persistence length, P, which is half the Kuhn length, is a commonly used alternative parameter. These parameters are related to the intrinsic chain elasticity parameter ϵ by $\lambda = kT/2\epsilon$. The transport and static properties of wormlike chain models have been reviewed recently by Yamakawa.[2] It is evident that the dynamics of these models is still in its development stage.

Harris and Hearst[3] were the first to propose a dynamical model of the wormlike chain treated as a differentiable space curve. This model has been criticized by Soda[4] for its internal inconsistencies. Nevertheless, it has been used in calculations of the forward depolarized dynamic scattering by Moro and Pecora[5] and extensively by Maeda and Fujime[6-8] to describe the polarized dynamic light scattering from semiflexible filaments. In a recent paper (hereafter referred to as I) Aragón and Pecora[9] presented a treatment of the dynamics of wormlike chains that is free of the inconsistencies of the Harris and Hearst model. By elim-

0024-9297/87/2220-0370$01.50/0

inating the stretching parameter from the theory and correctly enforcing the constraint of constant length, one is able to obtain a theory valid in the very rigid case. Yamakawa and Yoshizaki[10] have also presented a theory of the dynamics of the more general helical wormlike chain; however, only the static light scattering has been treated.[50]

In I, the polarized dynamic light scattering spectrum was calculated in the very flexible limit. In the present paper, a calculation of the forward depolarized dynamic light scattering is presented. The depolarized experiment is sensitive to reorientations of the optically anisotropic segments of the polymer molecules and thus is an excellent probe of the flexing degrees of freedom that interest us. The calculations described herein should also be applicable to the field-free decay of the induced birefringence for molecules with no net dipole moment.[11] The static depolarized light scattering from wormlike chains has been calculated by Nagai[12] and Allison.[13]

Whereas the theoretical basis for dynamic light scattering from rigid particles with arbitrary polarization and experimental geometry (including translation rotation coupling) has been well developed,[14] that for flexible molecules is still incomplete. In particular, the calculation of the depolarized light scattering spectrum has only been attempted in the forward scattering geometry.[5,15-18] The well-known theory of Ono and Okano[15] predicts an equally weighted sum of Lorentzians, one for each normal mode of a Rouse–Zimm chain, and is in apparent disagreement with the experimental data on polystyrenes of Bauer et al.,[19] in which the spectrum appears to be dominated by the longest wavelength relaxation. Data of Han and Yu[20] on several million molecular weight polystyrene could be fit successfully to equally weighted sums of Lorentzians, however.

Moro and Pecora[5,16] have presented two attempts to understand the experiments by the introduction of polymer rigidity into the calculation. The models successfully showed an increase in the weights of the first few modes as the rigidity is increased, yet at the same time, the models are incapable of yielding the correct rigid rod limit. The calculation presented herein for the free-draining case corroborates the above effects of rigidity and in addition does yield the correct rigid rod limit. In the next sections we present the general theory and its main assumptions, the calculation of the relevant orientational and configurational ensemble averages, and, finally, a discussion of the relaxation weights and a comparison with depolarized light scattering measurements of fairly flexible polymers, recent Brownian dynamics simulations, and experiments on DNA fragments.

II. General Theory

A dilute solution containing N identical polymers with segmental optical anisotropy β has an electric field correlation function given by[21]

$$C_{HV}(t) = N\beta^2\langle\sum_{i,j}^{n} u_{zi}(t)u_{yi}(t)u_{zj}(0)u_{yj}(0)\exp[i\mathbf{q}\cdot(\mathbf{r}_i(t)-\mathbf{r}_j(0))]\rangle \quad (2.1)$$

where the ith segment has an orientation $\mathbf{u}_i(t)$ at time t. The linearly polarized incident beam is assumed to propagate in the x direction with incident polarization along the z axis and detected polarization along the y axis. In the forward scattering we study the system at zero momentum transfer, $q = 0$. Going over into a continuum of segments, we parametrize the chain by a contour position s, $-L/2 \le s \le +L/2$, for a contour length L. Then we can write

$$C_{HV}(t) = N\beta^2\int_{-L/2}^{L/2}ds\int_{-L/2}^{L/2}ds'\,\langle u_z(s,t)u_y(s,t)u_z(s',0)u_y(s',0)\rangle \quad (2.2)$$

where the orientation of the polymer at position s is given by the tangent vector $\mathbf{u}(s,t) = \partial\mathbf{r}(s,t)/\partial s$ with respect to a coordinate system fixed in the laboratory frame.

As discussed in I, when the space curve that represents the polymer bends, but does not stretch, the tangent vectors are unit vectors. Thus, their Cartesian components can be expressed in terms of spherical harmonics:

$$u_z u_y = -i(2\pi/15)^{1/2}[Y_{21}(\mathbf{u}) + Y_{2-1}(\mathbf{u})] \quad (2.3)$$

At this point we must recognize that the rotational degrees of freedom of the polymer as a whole must be taken into account separately from the internal bending degrees of freedom. This is easily visualized in the case of the slightly bending rod: the flexing motions cannot generate an end-over-end tumbling motion of the molecule. That the overall rotational degrees of freedom exist cannot be changed by varying the flexibility parameter of the theory.

As a consequence of the above, we must choose a convenient molecule-fixed coordinate system to which we will refer the bending motions of the chain. A suitable choice is a system (x',y',z') with the z' axis along the unit vector $\mathbf{u}(0)$ at the center of the chain. The molecule frame is rotated with respect to the laboratory frame and has an orientation $\Omega_t = (\alpha(t),\beta(t),\gamma(t))$ at time t. We may now relate the spherical harmonics that depend on segmental orientations in the laboratory frame to the spherical harmonics in the molecule frame by use of the Wigner[22] rotation matrices

$$Y_{lm}(\Omega_{lab}(t)) = \sum_{m'} D^{l}_{mm'}(\Omega_t)Y_{lm'}(\Omega_{mol}(t)) \quad (2.4)$$

Note that the segment orientation, $\mathbf{u}'(s,t)$ in the molecule frame is still time dependent due to internal motions of the polymer. With the above expressions, the correlation function becomes

$$C_{HV}(t) = N\beta^2(2\pi/15L^2)\times \int_{-L/2}^{L/2}ds\int_{-L/2}^{L/2}ds'\sum_{mm'}\langle Y_{2m}(\mathbf{u}'(s,t))Y_{2m'}(\mathbf{u}'(s',0))\rangle \times \langle[D^2_{m1}(\Omega_t) + D^2_{m-1}(\Omega_t)][D^{2*}_{m'1}(\Omega_0) + D^{2*}_{m'-1}(\Omega_0)]\rangle \quad (2.5)$$

We have assumed, in writing the above, that the reorientation of the molecule frame is uncorrelated with internal motions of the polymer so that the ensemble average has been factored into two independent terms. We give arguments to justify this assumption below.

III. Orientational Correlation Function

The polymer molecule will constitute, for a given momentary configuration, a general hydrodynamic body with three different rotational diffusion coefficients. However, when the body is elongated (i.e., on the stiff side) the internal motions are rapid compared to reorientation.[9] That is, the average transverse dimensions of the polymer configuration, having no preferential direction, are cylindrically symmetric. Thus it is permissible to view the polymer configuration as that of an effective ellipsoid of revolution whose hydrodynamic size depends on the persistence length of the polymer. As the persistence length decreases, the polymer becomes less elongated and the flexing motions are slower. Furthermore, the polymer is already more coiled so that it takes less time to cover all transverse directions. Thus, throughout the whole range of polymer configurations, from stiff rod to random coil, we will represent the polymer, admittedly in an approximate fashion, by a cylindrically symmetric object.

In view of this discussion, we may compute the orientational correlation function by assuming that the only rotations that are strongly coupled to flexing motions are precisely the transverse whole-body reorientations. For simplicity, the reorientation of the elongation axis will be taken to be uncoupled to the flexing motions. In addition, we note that at $q = 0$ there is no coupling of rotational and translational degrees of freedom.[14] To proceed we require the joint probability distribution for the orientation of a cylindrical hydrodynamic body with a rotational diffusion coefficient Θ perpendicular to its main elongation axis. This distribution is[21]

$$F(\Omega_t,t;\Omega_0) = (8\pi^2)^{-2}\sum_{JM}(2J+1)D^{J*}_{0M}(\Omega_t)D^{J}_{0M}(\Omega_0)e^{-J(J+1)\Theta t} \tag{3.1}$$

where the quantum number that specifies the projection of the angular momentum on the molecular z' axis has been set to zero in anticipation of the consequences of the assumed cylindrical symmetry.

The orientational correlation function, after integration over Ω_t and Ω_0, becomes

$$\langle [D^2_{m1}(\Omega_t) + D^2_{m-1}(\Omega_t)][D^{2*}_{m'1}(\Omega_0) + D^{2*}_{m'-1}(\Omega_0)]\rangle = {}^2/_5\delta_{m0}\delta_{m'0}e^{-6\Theta t} \tag{3.2}$$

Note that the quantity Θ depends on three polymer parameters: the length L, the ratio of Kuhn length to L, $a \equiv \lambda L$, and the effective polymer hydrodynamic diameter d, through the axial ratio, L/d.

What we have achieved at this point is an approximate way of dealing with the hydrodynamics of the polymer reorientation so as to avoid the explicit treatment of the coupling between reorientation and internal flexing modes. As such, this treatment mirrors that of Hagerman and Zimm[23] for the rotational diffusion of a wormlike coil. Near the rod limit, the reorientation around the long axis is highly coupled to the flexing modes; in the flexible case, the coupling is so great that it becomes difficult to distinguish these degrees of freedom. The exact treatment of this problem would require dealing with a time-dependent asymmetric rotor configuration, where the polarizability may not be diagonalizable in the reference frame in which the rotational diffusion tensor is diagonal. This would force us to consider configurational averages of five exponential terms with configuration-dependent time constants. The formulation would be exceedingly complex; thus we seek to investigate here the simplest model that still retains the basic physics of the problem.

IV. Internal Mode Correlation Function

Incorporating the result of the previous section yields an expression for the depolarized correlation function

$$C_{HV}(t) = \frac{N\beta^2}{15L^2}\left(\frac{4\pi}{5}\right)e^{-6\Theta t}\int_{-L/2}^{L/2}ds\int_{-L/2}^{L/2}ds' \langle Y_{20}(\hat{u}(s,t))Y^*_{20}(\hat{u}(s',0))\rangle \tag{4.1}$$

where the primes on the molecule frame quantities will be eliminated from now on for simplicity. The correct rigid rod limit is obtained from this equation by recognizing that in this case all $\mathbf{u}(s,t) = \hat{z}$ and that $Y_{20}(\hat{z}) = (5/4\pi)^{1/2}$.

In order to evaluate the remaining configurational correlation function, we extract the time dependence from the spherical harmonic so that we may use the equilibrium configurational distribution for a wormlike coil derived by Saito et al.[9,24] As a first step, recall the normal mode expansions and the inverse utilized in I:

$$\mathbf{r}(s,t) = \sum_{l=0}^{\infty}\mathbf{p}_l(t)q_l(s) \tag{4.2a}$$

$$\mathbf{u}(s,t) = \sum_{l=0}^{\infty}\mathbf{p}_l(t)\frac{d}{ds}q_l(s) \tag{4.2b}$$

$$\mathbf{p}_l = -\int_{-L/2}^{L/2}\hat{u}(s')v_l(s')\,ds'; \qquad v_l(s) = \int_{-L/2}^{s}ds'\,q_l(s') \tag{4.2c}$$

Since $\hat{u}$ is a unit vector, we can write $\hat{u} = \sum\mathbf{c}_mY_{1m}(\hat{u})$ and inverse relation $\mathbf{c}_m^*\cdot\hat{u} = (4\pi/3)Y_{1m}(\hat{u})$, where $\mathbf{c}_0 = \hat{z}(4\pi/3)^{1/2}$ and $\mathbf{c}_1 = \mathbf{c}_{-1}^* = (2\pi/3)^{1/2}(\hat{x} - i\hat{y})$. Thus we obtain

$$Y_{1m}(\hat{u}(s,t)) = (3/4\pi)\sum_{l=0}\mathbf{c}_m\cdot\mathbf{p}_l(t)\frac{d}{ds}q(s) \tag{4.3}$$

Now we express Y_{20} in terms of Y_{1m} using the inverse Clebsch–Gordan series[22]

$$Y_{20}(\hat{u}(s,t)) = (10\pi/3)^{1/2}\sum_{m_1m_2}C(112;m_1m_20)Y_{1m_1}(\hat{u}(s,t))Y_{1m_2}(\hat{u}(s,t))$$

so that the configurational average may be expanded as

$$\langle Y_{20}(\hat{u}(s,t))Y_{20}(\hat{u}(s',0))\rangle = \left(\frac{3}{4\pi}\right)^2(10\pi/3)^{1/2}\times \sum_{m_1m_2}\sum_{lk}\frac{d}{ds}q_l(s)\frac{d}{ds}q_k(s)C(112;m_1m_20)\langle\mathbf{c}_{m_1}\cdot\mathbf{p}_l(t)\mathbf{c}_{m_2}\cdot\mathbf{p}_k(t)Y_{20}(\hat{u}(s',0))\rangle \tag{4.4}$$

At this point we may substitute the general solution to the Langevin equation for the $\mathbf{p}_l(t)$ obtained in I

$$\mathbf{p}_l(t) = \mathbf{p}_l(0)e^{-\lambda_lt/\zeta} + e^{-\lambda_lt/\zeta}\int_0^t e^{\lambda_lt'/\zeta}\mathbf{A}_l(t')\,dt'/\zeta \tag{4.5}$$

and take into account that the configurational averages containing components of the random force $\mathbf{A}_l$ are zero. Substituting, in addition, the inverse expansion eq 4.2c and the connection to the spherical harmonics, we obtain

$$\langle Y_{20}(\hat{u}(s,t))Y^*_{20}(\hat{u}(s',0))\rangle = \sum_{lk}\frac{d}{ds}q_l \frac{d}{ds}q_ke^{-(\lambda_l+\lambda_k)t/\zeta}(10\pi/3)^{1/2}\sum_{m_1m_2}C(112;m_1m_20)\int_{-L/2}^{L/2}ds_1\int_{-L/2}^{L/2}ds_2\,v_l(s_1)v_k(s_2)\langle Y_{1m_1}(\hat{u}(s_1))Y_{1m_2}(\hat{u}(s_2))Y_{20}(\hat{u}(s'))\rangle \tag{4.6}$$

The final form of the correlation function can now be written down

$$C_{HV}(t) = \frac{N\beta^2}{15}e^{-6\Theta t}\sum_{l,k=0}^{\infty}a_{lk}b_{lk}(a)e^{-(\lambda_l+\lambda_k)t/\zeta} \tag{4.7}$$

where the weight coefficients are given by

$$a_{lk} \equiv L^2\int_{-L/2}^{L/2}ds\,\frac{d}{ds}q_l\frac{d}{ds}q_k \tag{4.8a}$$

$$b_{lk}(a) \equiv \frac{4\pi(2\pi/15)^{1/2}}{L^4}\int_{-L/2}^{L/2}\int\int ds_1\,ds_2\,ds_3\,v_l(s_2)v_k(s_3)\times \sum_{m_1m_2}C(122;m_1m_20)\langle Y_{1m_1}(\hat{u}(s_2))Y_{1m_2}(\hat{u}(s_3))Y_{20}(\hat{u}(s_1))\rangle \tag{4.8b}$$

Equation 4.7 is the basic result of this paper. Note that $\lambda_0 = 0$ so that the first term in the sum is a purely rotational term.In practice, however, expressions for the coefficients will be needed so that one can know the number of relaxation terms that have to be considered in a given experiment. The functions q_l and v_l are given in Table I and the weights a_{lk} are given in Table II. These

Table I
Eigenfunctions of the Flexing Problem

parity	$q_j(y)$	$v_j(y) \times x_j$
$j = 0$	$3^{1/2}y$	$3^{1/2}(y^2 - 1)/4^a$
odd	$\cos(z_j y)/\cos(z_j) + \cosh(z_j y)/\cosh(z_j)$	$\sin(z_j y)/\cos(z_j) + \sinh(z_j y)/\cosh(z_j)$
even	$\sin(z_j y)/\sin(z_j) + \sinh(z_j y)/\sinh(z_j)$	$-\cos(z_j y)/\sin(z_j) + \cosh(z_j y)/\sinh(z_j)$

[a] This entry equals $v_0(y)$. $z_j = x_j/2$. $x_0 = 0$.

Table II
Weights a_{jk}

(j,k)	a_{jk}
0,0	12
0,k	$8(3^{1/2})$, k even
j,j	$4z_j^2[\cot^2(z_j) + 3\cot(z_j)/z_j]$, j even
j,j	$4z_j^2[\tan^2(z_j) - 3\tan(z_j)/z_j]$, j odd
j,k	$16[z_j z_k/(z_j^4 - z_k^4)][z_j^3\cot(z_k) - z_k^3\cot(z_j)]$, j, k even
j,k	$16[z_j z_k/(z_j^4 - z_k^4)][z_k^3\tan(z_j) - z_j^3\tan(z_k)]$, j, k odd

functions are independent of the configuration parameters of the polymer. Note that $a_{jk} = 0$ unless $j + k$ is even. The evaluation of the b_{lk} weights is very tedious so it is relegated to Appendix A. Before discussing the results in full, we first show that it has the correct limits in the next section.

V. Limiting Forms: Rigid Rod and Random Coil

In Appendix A it is shown that b_{lk} has the following form:

$$b_{lk}(a) = \frac{1}{8}\int_{-1}^{1}dy_1\int_{-1}^{y_1}dy_2\int_{-1}^{y_2}dy_3\sum_{ijn}|\epsilon_{ijn}|v_i(y_j)v_k(y_n)\{\}_i \tag{5.1}$$

where ϵ_{ijn} is the totally antisymmetric symbol, $a = \lambda L$, and the curly brackets $\{\}_i$ are given by

$$\{\}_3 = e^{-a(y_1-y_2)}e^{-3a(y_2-y_3)}\left[\frac{1}{5} + \frac{2}{7}e^{-3a|y_3|} + \frac{18}{35}e^{-10a|y_3|}\right] \tag{5.2a}$$

$$\{\}_2 = \frac{1}{5}e^{-a(y_1-y_2)}e^{-a(y_2-y_3)}[1 + e^{-3a|y_3|}] + \frac{3}{35}e^{-3a(y_1-y_2)}e^{-6a(y_2-y_3)}[e^{-3a|y_3|} + 6e^{-10a|y_3|}] \tag{5.2b}$$

$$\{\}_1 = \frac{1}{5}e^{-3a(y_1-y_2)}e^{-a(y_2-y_3)}[1 + e^{-3a|y_3|}] + \frac{3}{35}e^{-3a(y_1-y_2)}e^{-6a(y_2-y_3)}[e^{-3a|y_3|} + 6e^{-10a|y_3|}] \tag{5.2c}$$

Rigid Rod Limit. In the rigid rod limit, $a \approx 0$; thus all expressions in curly brackets in eq 5.2 become 1. In this case, eq 5.1 can be manipulated to a simple form. Since the argument is now symmetric in all the indices, the integrals can be unnested (factors of 3! will cancel out in the process) to obtain

$$b_{lk}(0) = \frac{1}{4}\int_{-1}^{1}\int_{-1}^{1}\int_{-1}^{1}dy_1\,dy_2\,dy_3\,v_l(y_1)v_k(y_2) = \frac{\delta_{l0}\delta_{k0}}{12} \tag{5.3}$$

where we have used the fact that an integral of v_l is proportional to the second derivative of q_l and thus vanishes at $y = \pm 1$ by the boundary conditions of the problem and that $v_0(y) = 3^{1/2}(y^2 - 1)/4$. Substituting the value for $a_{00} = 12$ from Table II, one finds that the correlation function becomes

$$C_{HV}(t) = \frac{N\beta^2}{15}e^{-6\Theta t} \tag{5.4}$$

Table III
Weights $b_{jk}(\infty)$

(j,k)	$b_{jk}(\infty)$
0,0	$1/(60a^2)$, k even
0,k	$-3^{1/2}(z_k\cot(z_k) - 1)/(12a^2z_k^4)$
j,j	$[z_j\cot^2(z_j) - \cot(z_j)]/(24a^2z_j^3)$, j even
j,j	$[z_j\tan^2(z_j) + \tan(z_j)]/(24a^2z_j^3)$, j odd
j,k	$[z_k\cot(z_k) - z_j\cot(z_j)]/[6a^2(z_j^4 - z_k^4)]$, j, k even
j,k	$[z_j\tan(z_j) - z_k\tan(z_k)]/[6a^2(z_j^4 - z_k^4)]$, j, k odd

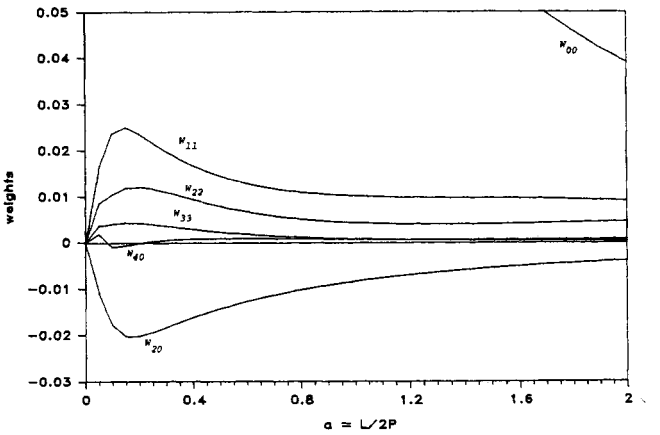

Figure 1. The weights w_{jk} as a function of $a = \lambda L = L/2P$. w_{00} goes off scale and is unity at $a = 0$, whereas all others start at zero, oscillate near zero, and decay as a grows large.

which is the correct limiting form for a rigid rod.[25]

Random Coil Limit. For the random coil, the persistence length becomes very small; thus we are interested in the limit $a \to \infty$. In order to evaluate this limit, we use the following property of the integrals, which can be easily proved by integration by parts. For a, $b > 0$

$$\lim_{a\to\infty}\left\{a\int_{-1}^{y}dx\,f(x)e^{-a(y-x)}\right\} = f(y) \tag{5.5a}$$

$$\lim_{a\to\infty}\left\{a\int_{-1}^{y}dx\,f(x)e^{-a(y-x)}e^{-ab|x|}\right\} = 0 \tag{5.5b}$$

Considering these relations, we see that the pieces of the argument of the $\{\}_i$ containing lone $\exp(-ma|y_3|)$ terms vanish in the limit. The remainder of the terms behave like Dirac δ functions and give

$$b_{lk}(\infty) = \frac{1}{12a^2}\int_{-1}^{1}dy\,v_l(y)v_k(y) \tag{5.6}$$

In this case the theory predicts that the full matrix of weight coefficients will contribute and all with very small intensity on account of the $1/a^2$ dependence. The above integrals can be evaluated analytically to give the results of Table III.

For intermediate values of a the full forms given in eq 5.1 were integrated. The first integral was done analytically, and the remaining double integral was done numerically with a Fortran implementation of Romberg quadrature.[26] The integration routine used a tolerance parameter such that the numbers could be computed to at least four significant figures.[27] The behavior of the total weight $w_{lk} = a_{lk}b_{lk}(a)$ is shown in Figure 1 as a function of a.

VI. Discussion and Conclusions

We have presented a theory of the foward depolarized light scattering from a dilute solution of free-draining wormlike chains. In order to simplify the calculation, we have assumed that the whole chain rotates in solution as a cylindrically symmetric effective hydrodynamic body.

The dynamical coupling of the flexing modes with the end-over-end tumbling has been ignored as have hydrodynamic and excluded volume interactions. The assumption is also made that the segmental polarizability is well-defined and of fixed orientation within each segment of the chain. This is a reasonable assumption for semirigid chains without bulky and floppy substituents.

In the following sections a proof of the positivity of the correlation function is discussed, and this work is compared to previous theoretical and experimental work.

(a) The Correlation Function Is Positive. One of the most striking aspects of the behavior of the weights is the fact that many of them are negative. The diagonal terms are always positive. The off-diagonal terms represent dynamically independent modes that are optically coupled. The negative sign implies that there exists an anticorrelation between modes of the same symmetry (note that all the modes have well-defined parity). It is quite acceptable to have some weights be negative as long as the total correlation function is positive at any time t. Correlation functions with negative terms have been shown to exist in depolarized scattering from coupled hydrodynamic modes in liquids of small molecules giving the well-known "Rayleigh dip" feature in the spectrum.[28]

As shown in Figure 1, the weight matrix, as a function of a, begins with the only nonzero element $w_{00} = 1$ at $a = 0$. As a increases, the diagonal and off-diagonal terms rapidly increase to maximum values between 1 and 3% of w_{00} at $a \simeq 0.2$ and thereafter decrease in magnitude as a continues to increase. The w_{00} term decreases at a faster rate than the remaining diagonal terms so that by $a \geq 10$, all diagonal terms have nearly the same intensity. The off-diagonal terms have decreased enough to be insignificant at these values of a. Taking into account that to a good approximation $\cot(z_j) \simeq 1$ (j even) and $\tan(z_j) \simeq -1$ (j odd, $z_j = x_j/2$), Tables II and III give the following expressions for the weights in the flexible case:

$$w_{00} = 1/5a^2$$

$$w_{0k} = \frac{2}{a^2 z_k{}^4}(1 - z_k)$$

$$w_{kk} = \frac{1}{6a^2}\left(1 + \frac{2}{z_k} - \frac{3}{z_k{}^2}\right)$$

$$w_{jk} = \frac{8 z_j z_k}{3a^2(z_j{}^4 - z_k{}^4)}(z_k - z_j)(z_j{}^3 - z_k{}^3) \qquad (6.1)$$

Utilizing these expressions it is possible to rigorously show that $w_{kk} > \sum_{j>k} w_{jk}$ so that the positive diagonal terms always dominate the sum of all off-diagonal terms on the same row. This implies, of course, that the correlation function is always positive since at $t > 0$, the contribution of the terms further away ($j > k$) decays faster. The complexity of the weight expressions for the intermediate values of a has frustrated a rigorous proof of the positivity of $C_{HV}(t)$ in that case. Nevertheless, since w_{00} is comparatively very large in that region, there is at least not an obvious problem.

(b) Previous Calculations. The first calculation of depolarized scattering from flexible polymers was that of Ono and Okano.[15] Utilizing the Rouse–Zimm model, their theory predicted an equally weighted sum of relaxing exponentials, i.e., a diagonal unit weight matrix w_{jk}. The calculation of Moro and Pecora,[5] using the Harris–Hearst model, gave a nondiagonal weight matrix that reduces exactly to the Ono–Okano result for very flexible chains and singles out the first term as the only surviving relaxation in the rigid limit, as does the theory presented here. The Harris–Hearst model achieves this with two parameters: one specifies harmonic stretching of the chain and the other is equivalent to ϵ, the elastic bending constant. However, as mentioned previously, this model is internally inconsistent. A subsequent calculation of Moro and Pecroa,[16] using projection operator techniques, gave results similar to the above except that only one stiffness parameter was required. Whereas the computed behavior of the weights in these theories has the sought-after behavior, the time constants make reference only to the flexing motions of the chain and thus can never describe the end-over-end tumbling of a rigid rod.

Other authors have introduced specialized models in an effort to understand the phenyl ring relaxation time observed in polystyrenes by Bauer et al.[19] (see below). Carpenter and Skolnick[17] have introduced the somewhat artificial mode of a straight rod with harmonic torsional degrees of freedom. Their computed correlation function contains unequally weighted and nondiagonal terms with a mixture of tumbling and Rouse–Zimm type time constants. It is not a good model for the description of flexural relaxations. Evans[18] has considered substituent bond polarizabilities and dipole–induced dipole interactions to produce correlation functions with two classes of relaxation times: one class corresponds to molecular weight independent high-frequency modes, and the other is a set of Rouse–Zimm modes. The presence of dipolar interactions gives these latter modes unequal weights. Without these interactions, however, Norisuye and Yu[29] have shown that under very general conditions, irrespective of the details of the dynamics, the existence of a normal mode decomposition and a mean square end-to-end distance proportional to the number of polymer segments (i.e., a very flexible chain), necessarily implies that the forward depolarized scattering will show equally weighted relaxations. Except for the last two calculations mentioned, all of the theoretical approaches discussed above have equally weighted relaxations in the flexible limit. The differences in the very flexible limit arise from the dynamics which specifies the nature of the relaxation times.

A treatment of the rotational diffusion of deformable macromolecules with mean local cylindrical symmetry has been given by Schurr.[30] Schurr has derived a general diffusion equation that applies when molecules can tumble, bend, and twist. In agreement with the treatment here, he recognizes that a molecule divided into N segments must be described by $3N + 1$ orientational variables of which 3 must be the Euler angles that specify overall rotation, regardless of the relative contributions of bending and overall rotation. Since we have not considered twisting degrees of freedom, we have used the tangent vectors $\mathbf{u}(s,t)$ in the molecule frame to specify the deformations at every point s on the chain and three Euler angles to specify the overall orientation of the body. The failure of the theories based on Rouse–Zimm models or the Harris–Hearst equation (in addition to the inconsistent treatment of the deformations in the latter) is due to the fact that the angular degrees of freedom relating the laboratory and the molecule frames have been ignored.

Schurr[30] gives detailed expressions for the twisting correlation function which are similar to the results of Skolnick et al.[17] but he does not treat the problem of tumbling and bending explicitly. This work is similar in spirit to the more general program of Yamakawa and Yoshizaki[10] for the helical wormlike coil. Their direct, and more difficult, approach permits the calculation of all correlation functions of interest. Since they have not ap-

plied their theory explicitly to the light scattering case, we reserve a detailed comparison with their work for a forthcoming communication on the fluorescence polarization anisotropy as calculated by our method.

Roitman and Zimm,[31] however, have made a detailed study of the rotational and flexing dynamics of the trumbell model. This model has very few degrees of freedom compared to a flexible molecule; nevertheless, the basic nature of the results is in agreement with our theory. They find that the slowest relaxational mode is nearly purely rotational whereas the faster relaxation is a mixed rotational–flexural mode. In addition, they also find that the rigid ensemble method of representing the rotational diffusion relaxation time is well justified over the whole range of flexibility of the trumbell. The largest error is 10–5% at the very flexible limit. This further supports the approach used here in which the configuration-dependent diffusion coefficient was replaced by that of the equivalent rigid body ensemble at each value of the flexibility parameter. We have argued, in addition, that this rigid ensemble is effectively cylindrically symmetric. This point needs to be investigated further in order to determine under what conditions other rigid body relaxations may significantly appear in the correlation function.

The time constants predicted by the present theory are very distinctive. The flexural time constants are given by[9]

$$\tau_j = \zeta/\lambda_j = (\zeta L^4)/(x_j{}^4\epsilon) = (2aL^2)/(Dx_j{}^4), \quad j = 1, 2, 3, \ldots \quad (6.2)$$

where the eigenvalue $\lambda_j = \epsilon x_j{}^4/L^4$, the translational diffusion coefficient $D = kT/L\zeta$, and the elasticity constant $\epsilon = kT/2\lambda$. Written in this way, the time constants are computable in terms of experimentally measurable parameters. The overall time constant for a given (jk) relaxation term, according to eq 4.7, is

$$\tau_{jk}{}^{-1} = 6\Theta(a) + \frac{D(a)}{2aL^2}(x_j{}^4 + x_k{}^4) \quad (6.3)$$

where we have emphasized the flexibility dependence of the two basic transport coefficients that enter. Utilizing theories of $\Theta(a)$ such as those by Yoshizaki and Yamakawa[32] or Hagerman and Zimm[23] and of $D(a)$ by Fujii and Yamakawa[33] which take hydrodynamic interactions into account, we can partially remedy this defect of the present theory (more about this aspect below). On the other hand, the time constants of the Rouse–Zimm theory are given by[34]

$$\tau_{jj}{}^{-1} = \frac{Dy_j}{2R_G{}^2}, \quad j = 1, 2, 3, \ldots \quad (6.4)$$

For the case of negligible hydrodynamic interaction, $y_j = \pi^2 j^2$. The value of the mean square radius of gyration for a flexible wormlike coil may be substituted to clarify the large differences, $R_G{}^2 = L^2/6a$. The theories of Moro and Pecora[5,16] give very similar forms where the off-diagonal terms contain the sum of $y_j + y_k$ and the values of these numbers depend on the flexibility parameter. The differences arise from the fact that the eigenvalue problem in our case is strictly that of a fourth-order operator and that the angular variables for overall rotation have been taken into account, giving a time constant that is the sum of three processes: one rotation plus two flexing modes.

(c) Analysis of the Very Flexible Case $a \geq 15$. The approximations involved in separating the flexing degrees of freedom from the whole-body rotations are least secure in the very flexible case. Nevertheless, it is instructive to push the present theory to this limit to see what is predicts and how these predictions compare with experiment.

For a very flexible polymer we can obtain expressions for Θ and D. For D we choose the formula of Yamakawa and Fujii,[33] which is a more precise version of the original formula of Hearst and Stockmayer.[35] To order λd and $a^{-1/2}$, the YF formula is

$$D(a,\lambda d) = \frac{kT}{3\pi\eta L}[1.843a^{1/2} - \ln(\lambda d) - 1.0561 - 0.1667\lambda d + 0.1382a^{-1/2}], \quad a > 10, \lambda d < 0.2 \quad (6.5)$$

For Θ we can use the Hearst formula[1]

$$\Theta(a,\lambda d) = \frac{kTa}{\eta L^3}[0.716a^{1/2} - 0.636\ln(\lambda d) - 0.908], \quad a \gg 1, \lambda d < 0.2 \quad (6.6)$$

The correlation function in the very flexible case is essentially diagonal so that the relevant time constant can be written as

$$\tau_{jj}{}^{-1} = 6\Theta[1 + c(2j+1)^4]t$$

$$c \equiv \frac{\pi^4 D}{96aL^2\Theta} = \frac{g(a,\lambda d)\pi^3}{112a^2} \quad (6.7)$$

and the function g is given by

$$g(a,\lambda d) = \frac{a^{1/2} - 0.543\ln(\lambda d) - 0.573}{a^{1/2} - 0.888\ln(\lambda d) - 1.27} \simeq 1 \quad (6.8)$$

Using eq 6.1 for the weights (ignoring the eigenvalue corrections since they will significantly affect only the first few terms), we obtain a simple form for the correlation function

$$C_{HV}(t) = \frac{1}{5}e^{-t'} + \frac{1}{6}\sum_{j=1}^{\infty} e^{-[1+c(2j+1)^4]t'} \quad (6.9)$$

where, for convenience, we have used a reduced time $t' = 6\Theta t$. The crucial observation at this point is that for large a, the *long-wave* flexing motions have become slower than the overall rotation of the coil. The increase in flexibility has enabled the coil to assume a much more compact hydrodynamic shape so that the quantity $c \ll 1$. This implies that many terms of the sum in eq 6.9 will contribute to the correlation function. Under these conditions it is suitable to approximate the sum in eq 6.9 by the Euler–MacLaurin summation formula,[36] which gives

$$\sum_{j=1}^{\infty} e^{-[1+c(2j+1)^4]t'} = \int_0^{\infty} e^{-[1+(2j+1)^4 t'}\,dj + 0.5e^{-(1+c)t'} + e^{-(1+c)t'}\left\{\frac{2ct'}{3} - \frac{8}{45}[8(ct')^3 + 24(ct')^2 - 3ct'] + \ldots\right\} \quad (6.10)$$

For $a \geq 15$, $c \leq 1.3 \times 10^{-3}$ so that $1 + c \simeq 1$ and the correction terms in parentheses contribute less than 0.5% and may be neglected (for $t' \leq 4$, the relevant time range). The integral can be evaluated exactly to give[37]

$$\int_0^{\infty} e^{-[1+(2j+1)^4]t'}\,dj = \frac{e^{-t'}}{2}\left\{0.25(ct')^{-1/4}\Gamma(1/4) - \sum_k \frac{(-)^k(ct')^k}{(4k+1)k!}\right\} \simeq 0.625a^{1/2}t'^{-1/4}e^{-t'} - 0.5e^{-t'} \quad (6.11)$$

The correlation function obtained from eq 6.9–6.11 has the final form

$$C(t') \simeq \frac{e^{-t'}}{30a^2}[1 + 3.12a^{1/2}t'^{-1/4}] \simeq t'^{-1/4}e^{-t'} \quad (6.12)$$

A plot of this function is shown in Figure 2, along with the single exponential for comparison. Equation 6.12 shows

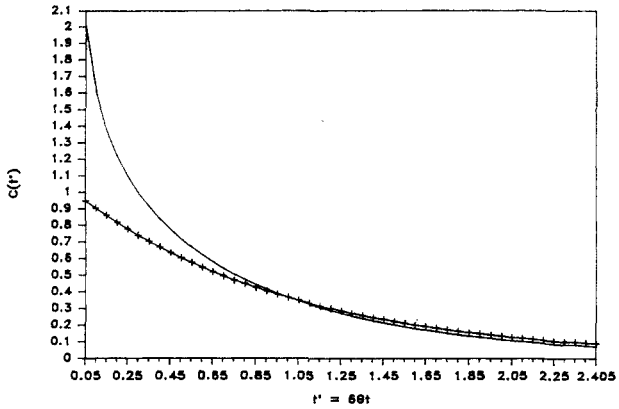

Figure 2. Correlation functions for the very flexible case. A single exponential (+), $\exp(-t')$, is compared to the predicted function, $\exp(-t')/t'^{1/4}$. Note the near-exponential tail.

that for large a, the shape of the correlation function is a universal function of t' and is characterized by pronounced curvature at small times and a near-exponential tail. These features can be understood qualitatively as follows. The correlation function has a large amplitude at $t' \simeq 0$ due to all modes being equally probable. This amplitude decays quickly as the many bending modes with large value of j relax. There remains, however, a set of low j modes that relax slower than rotation, and these constitute a slowly decreasing effective amplitude for the rotational decay. This explains the fact that the near-exponential tail in fact decays slightly faster than exponential.

It should be noted that unless the signal-to-noise ratio is very high, it would be impossible to distinguish an experimental curve of the predicted type from one due to 2–3 *unequally* weighted relaxations. Another experimental situation that may obscure this behavior is polydispersity. The effect of polydispersity is not very severe, however, since the very flexible chain rotational correlation times have an $L^{3/2}$ dependence compared to L^3 for a rigid rod. Moderate polydispersity should only make the characteristic features noted above less extreme but they should nevertheless remain.

In the case of the Ono and Okano[15] theory, a similar treatment can be carried out. For a very long chain, the Rouse eigenvalues are proportional to j^2 so that the Euler–MacLaurin summation formula gives a correlation function proportional to $t^{-1/2}$. For the Zimm[38] nondraining chain, the eigenvalues are approximately proportional to $j^{3/2}$ so that the summed correlation function behaves as $t^{-3/2}$. These functions diverge much faster than $t^{-1/4}$ and should be readily distinguishable from the behavior of eq 6.12. In particular, the results for the Rouse–Zimm model are completely independent of any parameters of the chain because these parameters have all become multiplicative factors with the overall scattering intensity.

There have been relatively few experiments of dynamic depolarized light scattering reported to date. A review has been presented recently by Zero and Pecora.[39] Experiments do not demonstrate the behavior $t^{-\alpha}$ ($0.5 < \alpha < 0.67$) predicted by the Rouse–Zimm models. In fact, all experiments, given the typical poor signal-to-noise ratio achievable in depolarized scattering, have shown that only a characteristic rotational time for the flexible polymer can be extracted from the data. That this should be possible with noisy data is clearly consistent with eq 6.12 but not with $t^{-\alpha}$ behavior.

Han and Yu[20] measured the forward depolarized scattering of isotactic polystyrene (PS, $M_w = 3.5 \times 10^6$, $\langle R_g^2 \rangle$ = 1270 Å) in THF and that of poly(hexyl isocyanate) (PHIC) for molecular weights up to 7.3×10^5 in *n*-hexane. Their data were taken with a spectrum analyzer and the signal-to-noise was not good, especially in the wings. For PS a value of $a = 735$ can be deduced from their data, whereas $a = 12$ for the largest PHIC. These values fall within the range of validity presented above. An unequivocal analysis was not possible; nevertheless, their data did suggest that the spectra were not single Lorentzian and that the equally weighted relaxations of the Rouse–Zimm model were not an optimum descriptor for the results.

Bauer et al.[19] (BBP) performed experiments on atactic polystyrene in tetrachloroethylene over a broad range of molecular weights. Molecular weights below 10^5 were studied by interferometry and, in addition to the slow relaxations of interest here, a weak fast (broad component in the spectrum) relaxation, independent of molecular weight, was also detected. This relaxation was attributed to local motions of the phenyl groups attached to the chain. The requirement of deconvoluting the instrumental line width in the presence of the broad component did not justify anything more than single-Lorentzian fits to the narrow component of the spectra. These gave relaxation times in accord with the first Rouse–Zimm mode, which corresponds to the overall tumbling of the coil in solution.

Samples of higher molecular weight up to 2×10^6 were also investigated by BBP using photon correlation spectroscopy at 2° scattering angle. Unfortunately, these data had much poorer signal-to-noise ratio than the interferometry data. For the highest molecular weight ($a > 1500$), the data did show evidence of nonexponential behavior in the form of excess curvature at short times. The correlation function fit well to a form containing effectively 2–3 exponentials with unequal weights. This, and the lack of positive evidence for the suitability of the Rouse–Zimm model, led the authors to conclude that their data were dominated by the longest wavelength relaxation in all cases. From the discussion above we see that this conclusion does not necessarily follow. The excess curvature is predicted by the present theory as the effective result of the contributions of many equally weighted relaxations. Furthermore, eq 6.12 predicts that a single-exponential fit will give a time constant very close to the effective tumbling relaxation of the whole chain, as was found from the data.

Jones and Wang[40] have reported a study of poly(propylene glycol) (PPG) of molecular weights 425, 1025, and 2025 in cyclohexane by interferometric depolarized light scattering at 90° scattering angle. The molecules are small enough that the experiment is equivalent to the forward depolarized geometry. In contrast to the experiments of BBP, the authors detected only one Lorentzian in their spectral data and interpreted it as segmental motion of the polymer backbone. The decay times where fit to a form $\tau = C\eta/T + \tau_0$, and the constant C was found to be independent of molecular weight. No interpretation was given for τ_0.

The data presented by these authors can be given an interpretation in terms of the normal modes of flexing of these molecules. The persistence length of polystyrene has been measured[41] in cyclohexane and is 13 Å. The persistence length of PPG should be somewhat smaller since there are no bulky side chains. If we use standard bond lengths and bond angles, the length of the extended-chain configuration for the PPG may be calculated. For example, the projected monomer length is 3.42 Å so that the 425 sample would have a length (extended chain) of 27.4 Å and a thickness $d = 3.1$ Å. Using the formula for $\Theta(a)$

of Yoshizaki and Yamakawa,[32] we find that the persistence length required to fit the measured time constant (taken as $1/6\Theta$) for PPG 425 is $p = 8.4$ Å, a very reasonable value. The raw data were extrapolated to zero concentration and the slip hydrodynamic boundary condition[42] was assumed in our estimation.

Thus, contrary to the author's claim, it is very reasonable to interpret the time constant for the smallest polymer as a whole-body rotation, yet of a somewhat flexible molecule. The next relaxation term would have been about 7 times faster and much weaker and not easily seen. For the larger sizes one immediately calculates that only the faster terms would give broad enough Lorentzians to be distinguishable from the instrumental line width. For example, using $p = 8.4$ Å, in the case of the 1025 polymer, $\tau_{22} = 0.69$ ns (0.79 ns, experiment) and for the 2025 polymer, $\tau_{55} = 1.56$ ns (1.24 ns, experiment), with all slower ones being undetectable (experimental data corrected as explained above). Thus the molecular weight independence of the data may only be apparent due to the varying modes observed at different molecular weights at the same temperature and different modes for the same molecular weight at different temperatures (the viscosity changed significantly with temperature). A plot of a specific relaxational mode time constant as a function of viscosity at constant temperature should have a zero intercept in dilute solution. To follow higher order modes individually, however, is probably not experimentally feasible in the very flexible case.

In summary, the available experimental data appear to show a surprising degree of consistency with the theory presented here.

(d) Comparison with Brownian Dynamics Simulations. Recent Brownian dynamics simulations of wormlike chains reported by Allison[43] provide a very interesting test of our theory at intermediate values of a. Allison has carried out simulations of a 30-bead chain with a persistence length $P = 400$ Å, a hydrodynamic diameter of 31.8 Å, and a contour length of 954 Å. These parameters are similar to ones observed for DNA. For this system $a \simeq 1.2$. During the simulation, the ensemble average, $G(t)$, of the product of Legendre polynomials $P_2(u_i(0))P_2(u_j(t))$ was computed and summed for all pairs i,j of beads on the chains. This ensemble average is the equivalent to eq 2.1 when $q = 0$. The results were presented as a plot of $g(t) = -\ln [G(t)/G(0)]$ as a function of t. At long times this function should have a slope of 6Θ, or unity in reduced time units.

A theoretical expression for $g(t)$ from eq 4.7 is

$$g(t) = 6\Theta t - \ln \left\{ \frac{\sum_{jk} w_{jk}(a) e^{-t/\tau_{jk}}}{\sum_{jk} w_{jk}(a)} \right\} \qquad (6.13)$$

where w_{jk} is the total weight and the time constant τ_{jk} is given by eq 6.3. When carrying out this evaluation in reduced time units, we need the quantity $D/(12aL^2\Theta) = 5.57 \times 10^{-3}$ at $a = 1.2$. From the YF[33] theory we obtained $D = 1.8 \times 10^{-7}$ cm^2/s, and from the theory of Hagerman and Zimm[23], $\Theta = 2.48 \times 10^4$ s^{-1} ($T = 293$ K, $\eta = 1.002$ cP). The sums in eq 6.13 were truncated after the first 10 terms. Several quantities relevant to the computation are given in Table IV.

The comparison of the theory with the simulation is shown in Figure 3. The theory does very poorly in reproducing the simulation data. In addition, as shown in Appendix C, the initial slope of $g(t)$ (the first cummulant) is very large and diverges for the very flexible case. The consequence of this is that the theoretical curve reaches the region of unit slope very quickly and thus the points

Table IV
Parameters Used in $g(t')$ at $a = 1.2$

(jk)	$w_{jk} \times 10^3$	$x_j^4 + x_k^4$	$w''_{jk} \times 10^3$	$w'_{jk} \times 10^3$
(0,0)	85.6	0	82	82
(1,1)	9.89	1001	50	20
(0,2)	−7.19	3797	0	10
(2,2)	4.22	7595	13.5	8
(1,3)	−9.17	15141	0	0.5
(0,4)	5.91	39976	0	1.4
(3,3)	0.98	29282	4	0.3
(2,4)	−0.276	43776	0	0.01
(1,5)	0.280	89635	0	0.1
(0,6)	−0.680	173880	0	0.02

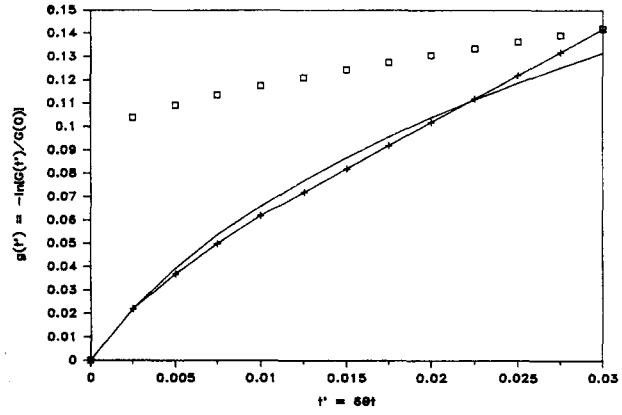

Figure 3. Comparison with Brownian dynamics simulations. The squares are values predicted by the free-draining theory. A different distribution of weights compares well with Allison's (+) results. See text for explanation.

shown in Figure 3 actually lie above $g(t') = 1$. For display purposes only, the theoretical values have been shifted down by $\simeq 0.9$. The third curve in Figure 3, which follows Allison's results very closely was computed with the weights w''_{jk} of Table IV. Many such sets of weights can give very similar curves (for example, the column labeled w'_{jk}), the main requirement being that the first few faster relaxations contribute more than the theory predicts. These arbitrary numbers have been introduced only to show that the problem does not appear to lie in the time constants but rather in the weights themselves.

The crucial difference with the simulations is that these have taken hydrodynamic interactions into account. The presence of the hydrodynamic interaction will definitely change the pattern of the weights since it will tend to couple the modes dynamically. Barkley and Zimm[44] have shown, for example, that the hydrodynamic interaction introduces mode dependent effective friction coefficients for the chain segments. This will tend to destroy the anticorrelations that have given rise, in the perfectly noninteracting case, to the negative weights. Maeda and Fujime[8] have presented a treatment of the hydrodynamic interaction for the wormlike coil. They have shown that the theory is quasi-diagonal in the slightly bendable case and in the very flexible case. Their analysis needs to be extended to intermediate values of λL since it is not clear that such behavior persists there also. In addition, it was noted that the eigenvalues of the problem change much less than the eigenfunctions so that a first-order perturbation treatment will suffice to correct the time constants. Much more work needs to be done on this aspect of the problem.

(e) Intermediate Flexibility $1 < a < 10$. The technique of transient electric birefringence[11] as applied to monodisperse DNA restriction fragments[45] has yielded high-quality data in which several relaxation processes can be resolved. As a final test of the theory, we will analyze

Table V
Analysis of the DNA Data of LPE[46]

DNA	τ_0, μs (P, Å)	τ_1, μs	τ_2, μs	τ_0/τ_1
367 bp	14.4–14[a]	2.3–2.0[a]	—	6.8–5.3[a]
L = 1233 Å	(574 ± 16)	1.87–1.8	0.28–0.26	8.0–7.5
L/P = 2.15 ± 3%				
762 bp				
L = 2560 Å	78–75[a]	18.0–16.5[a]	4–2[a]	5.6–4.0[a]
L/P = 3.42 ± 2%	(748 ± 18)	18.7–19.2	3.1–3.2	4.2–3.9
1010 bp				
L = 3394 Å	179–171[a]	40–37[a]	6–5[a]	4.8–3.8[a]
L/P = 3.2 ± 3%	(1058 ± 33)	41.0–39.7	6.9–6.5	4.5–4.2
2311 bp				
L = 7765 Å	688–670[a]	204–170[a]	60–40[a]	4–3[a]
L/P = 8.9 ± 1.1%	(870 ± 10)	458–454	145–142	1.5

[a] Experimental data.

the recent data of Lewis et al.[46] (LPE).

LPE have studied four samples of monodisperse DNA ranging from 367 to 2311 base pairs by dynamic birefringence. They have been able to resolve up to three relaxation processes in the data of DNA fragments, and comparisons were made with several theoretical models. In comparing the extracted time constants to the theory presented in I, LPE, in their simplified analysis, have apparently interpreted the time constants as being due to only one process: either rotation or flexing. However, as shown in eq 6.3, only the first time constant is a pure rotation. The remaining relaxation times are a mixture of rotational and flexural processes.

The data presented by LPE show a well-defined electric field pulse length dependence of the relative weights of the relaxations detected. Thus, in view of this and the previous discussions, our theoretical weights are not expected to apply. We will proceed to compare the prediction of the theory, assuming that the diagonal terms dominate, in terms of ratios of time constants given by

$$\tau_{jj}/\tau_{00} = \frac{1}{1 + bx_j^4}, \qquad b = \frac{D}{6aL^2\Theta}$$

$$\tau_{jj}/\tau_{kk} = \frac{1 + bx_k^4}{1 + bx_j^4} \tag{6.14}$$

In order to compute the quantity b we may use the YF[33] theory for D and the YY[32] theory for Θ. The Hagerman–Zimm theory differs by at most 5%, in the ranges of L/P of interest here, from the YY theory for Θ but cannot be applied to the largest fragment. The experimental data are not precise enough to distinguish between these theories in the regions where they both apply.

The analysis presented in Table V assumes the following values (taken from the LPE paper): 3.36 Å/base pair, d = 26 Å, T = 20 °C, η = 1.0 cP. As a first step, a range of persistence lengths was calculated from the observed range of rotational decay times and the YY theory. The experimental data and the results of this calculation are shown in column 2 of Table V. As LPE have noted, the persistence length is a function of contour length. Using eq 6.14 and the range of persistence lengths compatible with the range of rotational decay times allowed computation of the times predicted for the next two modes. Table V shows the experimental and the computed ranges for these quantities. It is evident that, except for the largest DNA, the agreement is good. The experimental data for the largest DNA were only partially resolved and have much more uncertainty than indicated. The fact that the assigned persistence length of this DNA is smaller than that of the previous size is indicative that something is not quite right. However, if we assume that P = 1000 Å, then the predicted times for the first four relaxations are 790, 480, 134, and 40 μs. The first two do not differ by a factor of 2 so it is reasonable to expect that the average, around 635 μs, would be observed, experimentally, instead. Thus it is quite possible that the lack of agreement between the theoretical prediction at $P \simeq 1000$ Å and the experimental values of the 2311 bp fragment simply reflects the lack of resolution in the data for the largest DNA.[51]

The general trends of the data are predicted very well by the theory, contrary to the initial assessment by LPE on the basis of certain aspects of the theory presented in I. In particular, the predicted ratio τ_1/τ_0 does not have an effective L^4 dependence when suitable transport coefficients are included in eq 6.14; thus the spacing of the modes, as well as their effective length dependence, agrees with experiment.

In conclusion, it appears that the present theory contains the basic elements for a consistent description of the time constants that enter in the q = 0 depolarized light scattering case and of the field-free decay of the transient electric birefringence. The most serious defect of the theory arises from the neglect of the hydrodynamic interactions, which are expected to modify the weights of the relaxation terms considerably and the time constants only to a small extent. This aspect is reserved for future work, as are applications to other experiments sensitive to flexural motions such as fluorescence polarization anisotropy, polarized dynamic light scattering, and NMR relaxation. The theory, as it stands, can already give substantial guidance, heretofore lacking, in the interpretation of flexural internal mode relaxations and their utilization for the study of polymer persistence length.

Acknowledgment. The author gratefully acknowledges support from a Fulbright–Hayes Fellowship and the stimulating hospitality of Professor Robert Pecora at Stanford University during the early stages of this work. Support from Universidad del Valle de Guatemala, where all the computations were done, is also gratefully acknowledged. The author thanks Professor Don Eden for helpful discussions.

Appendix A: Evaluation of Weight Coefficients

The first step in the evaluation of the b_{jk} coefficient according to eq 4.8b is the computation of the configurational average of three spherical harmonics. This can be accomplished with the use of the Green function $G(\Omega,\Omega';s-s')$, which specifies the probability that a segment at position s has an orientation Ω given that a segment at position s' has an orientation Ω′. Since the Green function requires that $s \geq s'$, we would first like to symmetrize the argument of the integral by introducing all permutations of the dummy variables s_i and dividing by their number since each permutation gives the same result. Now that the argument is symmetric, we can nest the integrals and multiply by 3! since we only integrate over 1/3! of the volume of a cube when nesting. Expressing the result in dimensionless variables $y_i = 2s_i/L$, we have

$$b_{lk}(a) = \frac{1}{8}\int_{-1}^{1}dy_1\int_{-1}^{y_1}dy_2\int_{-1}^{y_2}dy_3\sum_{ijn}|\epsilon_{ijn}|v_l(y_j)v_k(y_n) \times 4\pi(2\pi/15)^{1/2}\sum_{m_1m_2}C(112;m_1m_2 0)\langle Y_{1m_1}(\Omega_j)Y_{2m_2}(\Omega_n)Y_{20}(\Omega_i)\rangle \tag{A.1}$$

When we evaluate the configurational average of three spherical harmonics we notice that the coefficient $C(112;m_1m_20)$ is symmetric with respect to exchange of m_1,m_2 and therefore an exchange of j,n leaves the average unchanged. Thus, out of the six permutations, only three distinct ones need to be considered, say (123), (132), and (321). We present here the outline of the calculation of the (132) permutation and quote the results for the other cases.

In order to evaluate $\langle Y_{1m_1}(\Omega_j)Y_{1m_2}(\Omega_n)Y_{20}(\Omega_i)\rangle$ we start by specifying the probability that the segment at y_3 has orientation Ω_3 given that the reference element at $y = 0$ points along $\hat{z}'$. Then multiply by the probability that at y_2 the orientation is Ω_2 given that at y_3 it was Ω_3, and so on. Thus the average is evaluated by $\langle Y_{1m_1}(\Omega_j)Y_{1m_2}(\Omega_n)Y_{20}(\Omega_i)\rangle = \int\int\int d\Omega_3\ d\Omega_2\ d\Omega_1\ G(\Omega_3,\hat{z}';|y_3|)G(\Omega_2,\Omega_3;y_2-y_3)G(\Omega_1,\Omega_2;y_1-y_2)Y_{1m_1}(\Omega_j)Y_{1m_2}(\Omega_n)Y_{20}(\Omega_i)$. The Green function has the form[9]

$$G(\Omega,\Omega';y-y') = \sum_{lm} e^{-l(l+1)a|y-y'|}Y_{lm}(\Omega)Y_{lm}(\Omega') \quad \text{(A.2)}$$

and the integral over three spherical harmonics is[22]

$$\int d\Omega\ Y^*_{l_3m_3}(\Omega)Y_{l_2m_2}(\Omega)Y_{l_1m_1}(\Omega) = \left[\frac{(2l_1+1)(2l_2+1)}{4\pi(2l_3+1)}\right]^{1/2} C(l_1l_2l_3;m_1m_2m_3)C(l_1l_2l_3;000) \quad \text{(A.3)}$$

Using these expressions, we obtain, for example

$$\langle Y_{1m_1}(\Omega_1)Y_{1m_2}(\Omega_3)Y_{20}(\Omega_2)\rangle = (-1)^{m_1}e^{-a(y_1-y_2)} \times \sum_{r'}\left[\frac{15}{4\pi(2r'+1)}\right]^{1/2} C(21r';0-mn)C(21r';000) \times \sum_{r''}\left[\frac{3(2r''+1)}{4\pi(2r'+1)}\right]^{1/2} C(1r''r';m_20n)C(1r''r';000) \times \left[\frac{2r''+1}{4\pi}\right]^{1/2} e^{-r'(r'+1)a(y_2-y_3)/2}e^{-r''+1)a|y_3|/2} \quad \text{(A.4)}$$

If we now multiply by $4\pi(2\pi/15)^{1/2}\sum C(112;m_1m_20)$ and evaluate all the Clebsch–Gordan coefficients, we obtain eq 5.2b for $\{\}_2$. The rest of equations (5.2) are evaluated in a similar fashion, the permutation (123) giving $\{\}_3$ and (321) giving $\{\}_1$.

Appendix B: Total Scattering Intensity

The total scattering intensity is the zero-time value of the correlation function. This value can be computed directly by means of the Green function in eq A.2. From eq 2.2 and 2.3 we can write (using dimensionless variables)

$$C_{HV}(0) = \frac{\pi N\beta^2}{30}\int_{-1}^{1}\int_{-1}^{1} dy\ dy'\ \langle[Y_{21}(\Omega) + Y_{2-1}(\Omega)] \times [Y^*_{21}(\Omega') + Y^*_{2-1}(\Omega')]\rangle \quad \text{(B.1)}$$

The average over the spherical harmonics is performed by integrating over Ω and Ω' using eq A.2. The result is simply $\exp(-3a|y-y'|)/2\pi$. The double integral can be evaluated by changing variables and converting it into a single integral

$$C_{HV} = \frac{2N\beta^2}{15}\int_0^1 dx\ (1-x)e^{-6ax} = \frac{N\beta^2}{45}[1 + (e^{-6a}+1)/6a] \quad \text{(B.2)}$$

An equivalent form was obtained previously by Arpin et al.[47] The limiting behavior is easy to find:

$$C_{HV} = \beta^2/15 \quad \text{for } a = 0, \text{ rod}$$
$$C_{HV} = \beta^2/45a \quad \text{for } a = \infty, \text{ coil}$$

Appendix C: First Cummulant

For systems with complex correlation functions, it is often convenient to compute the first cummulant, Γ, defined by

$$\Gamma \equiv -\left.\frac{d\ln C(t)}{dt}\right|_{t=0} \quad \text{(C.1)}$$

Theoretically, one of the great advantages of the first cummulant is the fact that it can always be computed with the equilibrium distribution functions of the system.[48] It is apparently also easily experimentally accessible and is provided in data analysis packages in present-day commercial light scattering systems. Since the first cummulant represents the slope of the normalized correlation function at zero time, care must be taken in the interpretation of experimental values measured at finite times.[49]

In our case, the simplest starting point for its evaluation is eq 4.1. We can write down at once the following relation:

$$\Gamma = 6\Theta - \frac{4\pi}{5G(0)}\int_{-1}^{1}\int_{-1}^{1} dy\ dy'\left\langle\frac{dY_{20}}{du_z}\frac{du_z(y,t)}{dt}Y_{20}(\hat{u}(y',0))\right\rangle\Big|_{t=0} \quad \text{(C.2)}$$

where $C_{HV}(0) = N\beta^2G(0)/15$. Using the relations

$$\frac{dY_{20}}{du_z} = 15^{1/2}Y_{10}(\hat{u}) \quad \text{(C.3)}$$

$$\frac{du_z}{dt} = -(4\pi/3)^{1/2}\sum_j(\lambda_j/\zeta)\frac{dq_j}{dy}\int_{-1}^{1}dy''\ Y_{10}(\hat{u}(y''))v_j(y'') \quad \text{(C.4)}$$

where eq C.4 follows from eq 4.2, 4.3, and 4.5. Ignoring the random force term, we obtain

$$\Gamma = 6\Theta - \frac{4\pi}{5}(20\pi)^{1/2}\sum_j(\lambda_j/\zeta)\int_{-1}^{1}\int_{-1}^{1}\int_{-1}^{1}dy_1\ dy_2\ dy_3\ v_j(y_3)\frac{dq_j}{dy_1} \times \langle Y_{10}(u(y_1))Y_{20}(u(y_2))Y_{10}(u(y_3))\rangle/G(0) \quad \text{(C.5)}$$

The evaluation of this expression proceeds in identical fashion to the calculations described in Appendix A. The results are a

$$\Gamma = 6\Theta - \frac{D}{2aL^2}\sum_j x_j^4\int_{-1}^{1}\int_{-1}^{y_1}\int_{-1}^{y_2}dy_1\ dy_2\ dy_3\sum_{ilk}|\epsilon_{ilk}|v_j(y_l)\frac{dq_j}{dy_k}\{\}_i/G(0) \quad \text{(C.6)}$$

where we have introduced the translational diffusion coefficient into the time constant ζ/λ_j. The curly brackets are given by

$$\{\}_3 = e^{-a(y_1-y_2)}\left\{e^{-3a|y_3|} + 2e^{-3a(y_2-y_3)}\left[\frac{1}{5} + \frac{2}{7}e^{-3a|y_3|} + \frac{18}{35}e^{-10a|y_3|}\right]\right\}$$

$$\{\}_2 = \frac{1}{5}e^{-a(y_1-y_2)}\left\{2e^{-a(y_2-y_3)}[1 + 2e^{-3a|y_3|}] + \frac{9}{7}e^{-6a(y_2-y_3)}[3e^{-3a|y_3|} + 4e^{-10a|y_3|}]\right\}$$

$$\{\}_1 = \frac{1}{5}e^{-3a(y_1-y_2)}\left\{2e^{-a(y_2-y_3)}[1 + 2e^{-3a|y_3|}] + \frac{9}{7}e^{-6a(y_2-y_3)}[3e^{-3a|y_3|} + 4e^{-10a|y_3|}]\right\} \quad \text{(C.7)}$$

The rod and coil limits are easily obtained. For the rod case, all $\{\}_l = 3$ and the integral can be unnested. The integrals of v_l vanish for $l \neq 0$ so that $\Gamma = 6\Theta$, as expected. In the coil limit, as described by eq 5.5, the surviving terms add to give

$$\Gamma = 6\Theta - \frac{2D}{3aL^2}\sum_{l=1}^{\infty} x_l^4 \int_{-1}^{1} dy\, v_l(y)\, \frac{dq_l(y)}{dy} \qquad (C.8)$$

The remaining integral can be evaluated by integration by parts and it can be shown, utilizing the properties of v_l and q_l, that it has the value -1 for all l. Thus, recalling that $x_l \simeq (2l + 1)\pi/2$, we have the not too surprising result that the first cummulant, in the very flexible limit, diverges. The continuous Kratky–Porod model is unphysical insofar as it contains an infinite number of modes. A real chain cannot flex on scales less than a bond length so that the expansion should actually contain a cutoff at some suitably small wavelength.

References and Notes

(1) Yamakawa, H. *Modern Theory of Polymer Solutions*; Harper and Row: New York, 1971.
(2) Yamakawa, H. *Annu. Rev. Phys. Chem.* **1984**, *35*, 23.
(3) Harris, R. A.; Hearst, J. E. *J. Chem. Phys.* **1966**, *44*, 2595. Hearst, J. E.; Harris, R. A.; Beals, E. *J. Chem. Phys.* **1966**, *45*, 3106; **1967**, *46*, 398.
(4) Soda, K. *J. Phys. Soc. Jpn.* **1973**, *35*, 866.
(5) Moro, K.; Pecora, R. *J. Chem. Phys.* **1978**, *69*, 3254.
(6) Maeda, T.; Fujime, S. *Macromolecules* **1981**, *14*, 809.
(7) Maeda, T.; Fujime, S. *Macromolecules* **1984**, *17*, 1157, 2381.
(8) Fujime, S.; Maeda, T. *Macromolecules* **1985**, *18*, 191. Maeda, T.; Fujime, S. *Macromolecules* **1985**, *18*, 2430.
(9) Aragón, S. R; Pecora, R. *Macromolecules* **1985**, *18*, 1868.
(10) Yamakawa, H.; Yoshizaki, T. *J. Chem. Phys.* **1981**, *75*, 1016; **1983**, *78*, 572; **1984**, *81*, 982. Yamakawa, H.; Fujii, M. *J. Chem. Phys.* **1984**, *81*, 997.
(11) See, for example: Eden, D.; Elias, J. G. In *Measurement of Suspended Particles by Quasi-elastic Light Scattering*; Dahneke, B., Ed.; Wiley: New York, 1983.
(12) Nagai, K. *Polym. J. (Tokyo)* **1972**, *3*, 67.
(13) Allison, S. A. *Biopolymers* **1983**, *22*, 1545; **1984**, *23*, 607.
(14) Aragón, S. R.; Pecora, R. *J. Chem. Phys.* **1985**, *82*, 5346.
(15) Ono, K.; Okano, K. *Jpn. J.* Appl. *Phys.* **1970**, *9*, 1356.
(16) Moro, K.; Pecora, R. *J. Chem. Phys.* **1980**, *72*, 4958.
(17) Carpenter, D. K.; Skolnick, J. *Macromolecules* **1981**, *14*, 1284.
(18) Evans, G. T. *J. Chem. Phys.* **1979**, *71*, 2263.
(19) Bauer, D. R.; Brauman, J. I.; Pecora, R. *Macromolecules* **1975**, *8*, 443.
(20) Han, C.-C.; Yu, H. *J. Chem. Phys.* **1980**, *72*, 4958.
(21) Berne, B. J.; Pecora, R. *Dynamic Light Scattering with Applications to Chemistry, Biology and Physics*; Wiley-Interscience: New York, 1976.
(22) Rose, M. E. *Elementary Theory of Angular Momentum*; Wiley: New York, 1957.
(23) Hagerman, P.; Zimm, B. *Biopolymers* **1981**, *20*, 1481.
(24) Saito, N.; Takahashi, K.; Yunoki, Y. *J. Phys. Soc. Jpn.* **1967**, *22*, 219.
(25) Pecora, R. *J. Chem. Phys.* **1968**, *49*, 1036.
(26) Ralston, A.; Wilf, H. S. *Mathematical Methods for Digital Computers*; Wiley: New York, 1967; Vol. II.
(27) The numerical work was done on an HP-3000 Series 40 minicomputer at Universidad del Valle de Guatemala, Guatemala.
(28) Alms, G. R.; Bauer, D. R.; Brauman, J. I.; Pecora, R. *J. Chem. Phys.* **1973**, *59*, 5305, 5310.
(29) Norisuye, T.; Yu, H. *J. Chem. Phys.* **1978**, *68*, 4038.
(30) Schurr, J. M. *Chem. Phys.* **1984**, *84*, 71.
(31) Roitman, D. B.; Zimm, B. H. *J. Chem. Phys.* **1984**, *81*, 6333, 6348.
(32) Yoshisaki, T.; Yamakawa, H. *J. Chem. Phys.* **1984**, *81*, 982.
(33) Yamakawa, H.; Fujii, M. *Macromolecules* **1973**, *6*, 407. Nosisuye, T.; Motokowa, M.; Fujita, H. *Macromolecules* **1979**, *12*, 320.
(34) Zimm, B. H. *J. Chem. Phys.* **1956**, *24*, 269.
(35) Hearst, J. E.; Stockmayer, W. H. *J. Chem. Phys.* **1962**, *37*, 1425.
(36) Arfken, G. *Mathematical Methods for Physicists*; Academic: New York, 1970.
(37) Gradshteyn, I. S.; Ryzhik, I. M. *Tables of Integrals, Series and Products*; Academic: New York, 1980.
(38) Zimm, B. H.; Roe, G. M.; Epstein, L. F. *J. Chem. Phys.* **1956**, *24*, 729.
(39) Zero, K.; Pecora, R. In *Dynamic Light Scattering*; Pecora, R., Ed.; Plenum: New York, 1985.
(40) Jones, D. R.; Wang, C. H. *J. Chem. Phys.* **1976**, *65*, 1835.
(41) Durschlag, H.; Kratky, O.; Brieterbach, J. W.; Wolf, B. A. *Monatsh. Chem.* **1970**, *101*, 1462.
(42) Hu, C. M.; Zwanzig, R. *J. Chem. Phys.* **1974**, *60*, 4354.
(43) Allison, S. A. *Macromolecules* **1986**, *19*, 118.
(44) Barkely, M. D.; Zimm, B. H. *J. Chem. Phys.* **1979**, *70*, 2991.
(45) Lewis, R. J.; Huang, J.; Pecora, R. *Macromolecules* **1985**, *18*, 1530.
(46) Lewis, R. J.; Pecora, R.; Eden, D. *Macromolecules* **1985**, *19*, 134.
(47) Arpin, M.; Strazielle, C.; Weill, G.; Benoit, H. *Polymer* **1977**, *18*, 262.
(48) Akcasu, Z.; Benmouna, M.; Han, C. C. *Polymer* **1980**, *21*, 866.
(49) Stockmayer, W. H.; Burchard, W. *J. Chem. Phys.* **1979**, *70*, 3138.
(50) Yamakawa, H.; Fujii, M.; Shimada, J. *J. Chem. Phys.* **1979**, *71*, 1611.
(51) A different point of view is expressed in: Lewis, R. J.; Pecora, R. *Macromolecules* **1986**, *19*, 2074.